有机化学 DOI: 10.6023/cjoc202206007 研究论文
Chinese Journal of Organic Chemistry ARTICLE

一种裸眼和荧光双通道快速检测 Hg^{2+} 的探针及其多种应用

唐宏伟 王 超 钟克利 侯淑华 汤立军* 边延江*
(渤海大学化学与材料工程学院 辽宁锦州 121000)

摘要 设计并合成了一种在二甲基亚砜(DMSO)/磷酸缓冲溶液(PBS) (V∶V=5∶5, pH=10.17)中识别 Hg^{2+} 的荧光探针 **HMI-Hg^{2+}**. **HMI-Hg^{2+}**通过荧光信号增强识别 Hg^{2+}, 并且溶液颜色在几秒钟内发生改变. 光谱实验证实了该探针对 Hg^{2+} 具有高选择性和高灵敏度, 检测限为 0.22 μmol/L. **HMI-Hg^{2+}**在水样和海鲜样品(鱼、虾和扇贝)中具有出色的检测效果. 此外, **HMI-Hg^{2+}**可用于在 MCF-7 细胞中对 Hg^{2+} 进行成像, 并具有线粒体靶向能力.
关键词 荧光探针; Hg^{2+}; 海鲜样品; 细胞成像

A Naked-Eye and Fluorescent Dual-Channel Probe for Rapid Detection of Hg^{2+} and Its Multiple Applications

Tang, Hongwei Wang, Chao Zhong, Keli Hou, Shuhua
Tang, Lijun* Bian, Yanjiang*
(*College of Chemistry and Material Engineering*, *Bohai University*, *Jinzhou*, *Liaoning 121000*)

Abstract A fluorescent probe **HMI-Hg^{2+}** was designed and synthesized to recognize Hg^{2+} in dimethyl sulfoxide (DMSO)/phosphate buffer solution (PBS) (V∶V=5∶5, pH=10.17). **HMI-Hg^{2+}** recognized Hg^{2+} through the fluorescence signal strengthen, and solution color shifted within a few seconds. Spectral experiments confirmed the advantages of the probe with high selectivity and sensitivity to Hg^{2+}. The detection limit was calculated to be 0.22 μmol/L. **HMI-Hg^{2+}** has excellent detection consequences in water samples and seafood samples (fish, shrimp and scallop). Moreover, **HMI-Hg^{2+}** can be applied for the cell imaging of Hg^{2+} in MCF-7 and has mitochondria-targeted capabilities.
Keywords fluorescent probe; Hg^{2+}; seafood sample; cell imaging

1 Introduction

Mercury (Hg^{2+}) is a well-known toxic heavy metal.[1] Mercury readily bioaccumulates through the food chain but is troublesome to bio-degrade in bodies.[2-4] At the same time, mercury contamination of water and aquatic organisms (such as fish) also threatens people's health.[5-6] Even trace amounts of Hg^{2+} can cause irreversible damage to human organs and the nervous system.[7-9] Contamination of water, soil and ecosystems by mercury in nature remains a problem that cannot be ignored.[10-12] Therefore, due to these environmental and health concerns, various techniques have been developed for monitoring Hg^{2+} content, such as electrochemical method,[13] inductively coupled plasma mass spectrometry,[14] atomic emission spectroscopy[15] and atomic absorption spectrometry.[16] Compared with these methods, fluorescence techniques are favored because they do not require expensive instrumentation and have advantages of convenience and high sensitivity.[17-19]

Several fluorescent probes have been reported to detect Hg^{2+}, among which probes designed based on specific reactions superior to other sensing mechanisms in terms of selectivity and sensitivity, most of these probes have achieved good results in emission wavelength, water solubility and bioimaging, but further exploration is needed in reaction speed and detection of actual samples.[20-25] Therefore, it is necessary to prepare a fluorescent probe with high sensitivity that can detect lower levels of Hg^{2+} in actual samples and organisms. In addition, the thioacetals deprotection mechanism is considered to be a favorable option.[26-28] In this work, a probe **HMI-Hg^{2+}** with a fast response to Hg^{2+} and favorable application results in actual samples was synthesized, which was based on Hg^{2+}-induced deprotection of dithioacetal to release aldehyde (Scheme 1).

* Corresponding authors. E-mail: ljtang@bhu.edu.cn; bianyanjiang@126.com
Received June 6, 2022; revised August 29, 2022; published online October 10, 2022.
Project supported by the National Natural Science Foundation of China (No. 22278038) and the Program for Distinguished Professor of Liaoning Province.
国家自然科学基金(No. 22278038)和辽宁特聘教授支持计划资助项目.

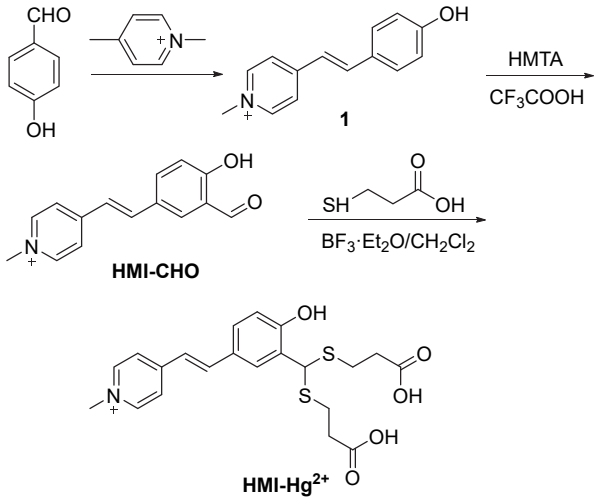

Scheme 1 Synthesis of probe **HMI-Hg^{2+}**

2 Results and discussion

2.1 Selectivity experiment of HMI-Hg^{2+}

The selectivity of UV absorption and fluorescence spectra for metal ions including Ba^{2+}, Fe^{2+}, Fe^{3+}, Mn^{2+}, Mg^{2+}, Hg^{2+}, Cu^{2+}, Zn^{2+}, Al^{3+}, Na^{+}, Cd^{2+}, Ni^{2+}, Ca^{2+}, Co^{2+}, Cr^{3+}, Pb^{2+}, K^{+} and Ag^{+} was investigated. As shown in Figure 1, the absorption wavelength of **HMI-Hg^{2+}** changed after the addition of Hg^{2+} and a new absorption peak appeared at 455 nm. In contrast, other metal ions had no significant effect on the absorption spectra of **HMI-Hg^{2+}**. Meanwhile, in the presence of Hg^{2+}, the **HMI-Hg^{2+}** solution exhibited a color change from light pink to yellow (Figure 2), which was clearly distinguishable from other metal ions. The selectivity experiment of **HMI-Hg^{2+}** on the fluorescence spectra of metal ions was carried out. As shown in Figure 3, we observed that **HMI-Hg^{2+}** has a weak fluorescence emission band at 602 nm, and the emission band changed slightly after adding Ag^{+}. When Hg^{2+} existed, the maximum emission wavelength was blue-shifted, and a new strong emission peak appeared at 585 nm. The specificity of **HMI-Hg^{2+}** for Hg^{2+} was also investigated by the fluorescence color changes, where strong orange fluorescence emission appeared only in the presence of Hg^{2+} (Figure 3 inset).

2.2 Titration experiment

Titration experiments with UV absorption spectroscopy were carried out. The color of **HMI-Hg^{2+}** transitioned from light pink to yellow with increasing Hg^{2+} concentration. In addition, when 1 equiv. of Hg^{2+} was added, the absorption wavelength gradually moved from 474 nm to 455 nm. We continued to explore the fluorescence titration experiments. When Hg^{2+} (0～12 μmol/L) was present in **HMI-Hg^{2+}**, the fluorescence intensity of **HMI-Hg^{2+}** gradually increased, and the maximum emission wavelength gradually blue-shifted to 585 nm. In addition, the fluorescence intensity of **HMI-Hg^{2+}** remained stable when 1.2 equiv. of Hg^{2+} was added (Figure 4a). And the fluorescence intensity of **HMI-Hg^{2+}** showed a favorable linear relationship with the added Hg^{2+} concentration (0～12 μmol/L) (R^2>0.99). The limit of detection was 0.22 μmol/L (LOD=3σ/k).[29-30] The results demonstrated that the response of **HMI-Hg^{2+}** to Hg^{2+} displayed gratifying sensitivity (Figure 4b).

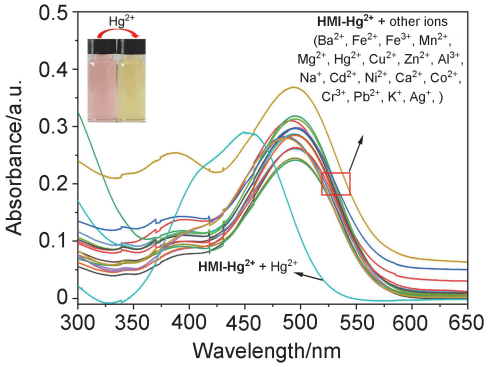

Figure 1 UV absorption spectra changes after metal ions (10 μmol/L) added to **HMI-Hg^{2+}** in DMSO/PBS (V∶V=5∶5, pH=10.17) solution (Inset: color changes of **HMI-Hg^{2+}** before and after addition of Hg^{2+} under sunlight)

Figure 2 Color changes of **HMI-Hg^{2+}** solution upon the addition of various metal ions under sunlight
0, **HMI-Hg^{2+}**; 1, Ba^{2+}; 2, Fe^{2+}; 3, Fe^{3+}; 4, Mn^{2+}; 5, Mg^{2+}; 6, Hg^{2+}; 7, Cu^{2+}; 8, Zn^{2+}; 9, Al^{3+}; 10, Na^{+}; 11, Cd^{2+}; 12, Ni^{2+}; 13, Ca^{2+}; 14, Co^{2+}; 15, Cr^{3+}; 16, Pb^{2+}; 17, K^{+}; 18, Ag^{+}.

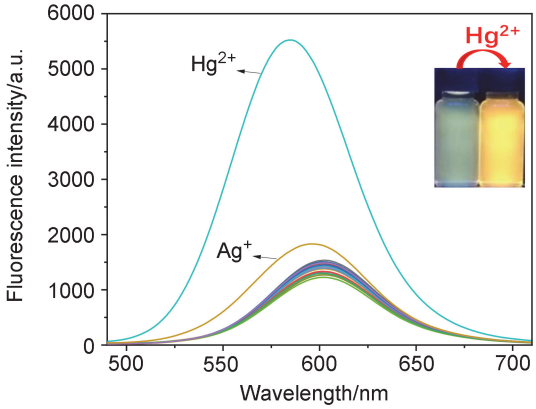

Figure 3 Fluorescence intensity changes after all kinds of ions (12 μmol/L) added to **HMI-Hg^{2+}**
Inset: fluorescence color changes of **HMI-Hg^{2+}** before and after addition of Hg^{2+} under UV lamp irradiation at 365 nm. λ_{ex}=455 nm, λ_{em}=585 nm.

2.3 Anti-interference experiment

The anti-interference ability of **HMI-Hg^{2+}** in complex environments was an essential criterion for measuring the practicability of probes. The fluorescence spectra of **HMI-Hg^{2+}** were investigated in the presence of various metal ions in solution and further coexisting with Hg^{2+}. As shown

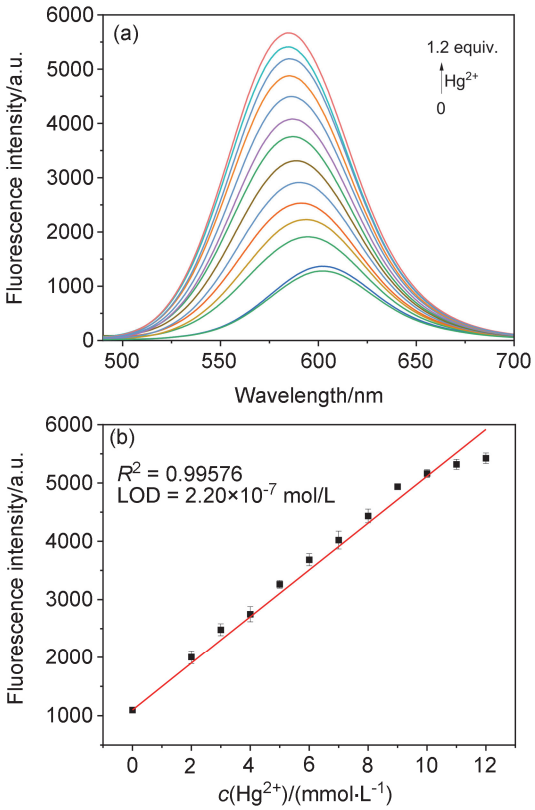

Figure 4 (a) Fluorescence intensity changes of **HMI-Hg^{2+}** after Hg^{2+} (0～12 μmol/L) gradually added and (b) linear relationship between the concentration of Hg^{2+} (0～12 μmol/L) added to **HMI-Hg^{2+}** and fluorescence intensity (λ_{em}=585 nm)

in Figure 5, fluorescence spectra of **HMI-Hg^{2+}** solution in the presence of various metal ions and further coexisting with Hg^{2+} were investigated. Various metal ions were added to **HMI-Hg^{2+}**, only that Hg^{2+} significantly enhanced the emission intensity at 585 nm. After adding Hg^{2+} in sequence, the emission intensity was distinctly intensified at 585 nm, indicating that the presence of other ions did not

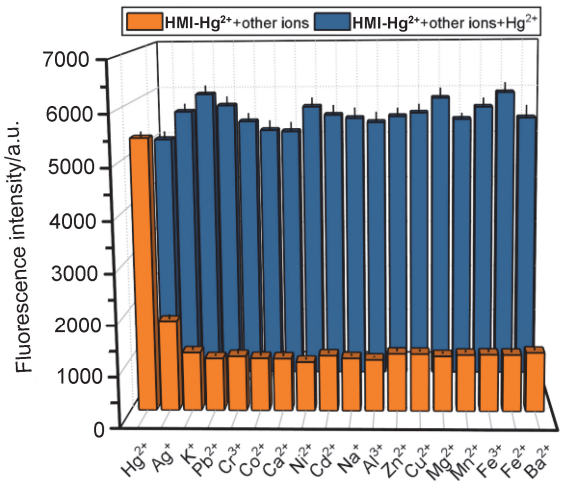

Figure 5 Fluorescence intensity changes when other ions (12 μmol/L) added to **HMI-Hg^{2+}** and Hg^{2+} (12 μmol/L) further added (λ_{em}=585 nm)

interfere with Hg^{2+}. In conclusion, **HMI-Hg^{2+}** had excellent anti-interference ability and great practical application prospects.

2.4 Effects of pH and time response

The fluorescence intensity changes of **HMI-Hg^{2+}** under different pH conditions were compared. In the absence of Hg^{2+}, **HMI-Hg^{2+}** had no fluorescence emission in the pH range of 2～8 and exhibited weak fluorescence emission in pH 9～13. In the presence of Hg^{2+}, in the pH range of 2～6, **HMI-Hg^{2+}** had no fluorescence emission. And under alkaline conditions, the emission intensity of **HMI-Hg^{2+}** enhanced conspicuously.

Hg^{2+} (12 μmol/L) was added to the **HMI-Hg^{2+}** solution and the mixture was immediately transferred to the cuvette to start the time scanning. In the existence of Hg^{2+}, the emission intensity of **HMI-Hg^{2+}** redoubled expeditiously and remained stable for about 6 s. In addition, we further verified this fast process with video. The results indicated that **HMI-Hg^{2+}** could potentially serve as a fast-response Hg^{2+} sensor.

2.5 Response mechanism of HMI-Hg^{2+} to Hg^{2+}

The mechanism of the probe **HMI-Hg^{2+}** to Hg^{2+} was shown in Scheme 2. To verify this mechanism, we compared the UV absorption and fluorescence spectra of **HMI-CHO** and **HMI-Hg^{2+}** with Hg^{2+} under the same system. The consistency proved that **HMI-Hg^{2+}** interacted with Hg^{2+} to remove the dithioacetal moiety and released **HMI-CHO**.[31] Meanwhile, the polarities of the compounds **HMI-CHO**, **HMI-Hg^{2+}** and the reaction mixture were compared by thin layer chromatography (TLC) under EtOH/CH_2Cl_2 (V∶V=1∶3) (Figure 6). Under UV light irradiation, the R_f values of **HMI-CHO** and the reaction mixture were similar, and both showed yellow-green fluorescence. Mass spectrometry results indicated a new peak at m/z 240.1017 (calcd 240.1019) assigned to $[M-I]^+$, which was consistent with the m/z of **HMI-CHO**. ^{1}H NMR of the isolated product was another sufficient evidence (Figure 7). The signal peaks b' (δ 5.46) and c' (δ 12.28) belonging to the dithioacetal moiety in the isolated product disappeared, and a new signal peak appeared at δ 10.32, which was assignable to the aldehyde proton (H_b).

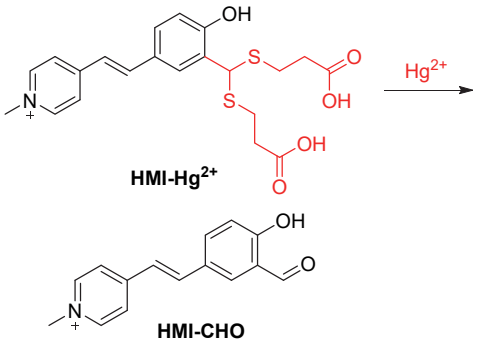

Scheme 2 Proposed mechanism of probe **HMI-Hg^{2+}** to Hg^{2+}

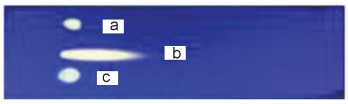

Figure 6 TLC plate tracer under 365 nm irradiation
(a) Compound **HMI-CHO**; (b) probe **HMI-Hg^{2+}**; (c) reaction mixture of **HMI-Hg^{2+}** with Hg^{2+}.

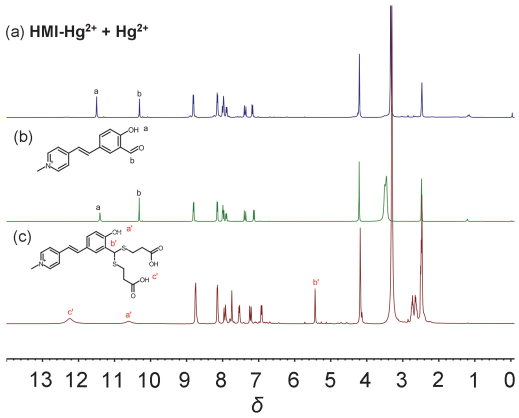

Figure 7 Comparison of partial ^{1}H NMR spectra of isolated product from reaction of **HMI-Hg^{2+}** with Hg^{2+}, compound **HMI-CHO** and **HMI-Hg^{2+}** in DMSO-d_6

2.6 Detection of Hg^{2+} in actual samples with **HMI-Hg^{2+}**

To study the practical application ability of **HMI-Hg^{2+}** in actual samples, the fluorescence properties of **HMI-Hg^{2+}** in lake and tap water samples were investigated. In the test solution of DMSO/H_2O (V∶V=5∶5), the fluorescence emission intensity at 585 nm was monitored. It was found that the fluorescence intensity had a better linear relationship with the concentration of Hg^{2+} spiked (R^2>0.99). We selected the low level of Hg^{2+} content to calculate the recovery rate of standard addition (Table 1). The recovery rate range is 93.4%～107.2%, and the relative standard deviations (RSDs) are between 1.52%～8.24%, indicating that **HMI-Hg^{2+}** can detect lower levels of Hg^{2+} in complex environments.

Table 1 Detection results of Hg^{2+} in water samples

Sample	Added/ (μmol•L^{-1})	Found/ (μmol•L^{-1})	RSD (n=3)/%	Recovery/%
Lake water	1	1.06	4.77	100.6
	2	1.82	3.99	93.7
	3	3.22	8.24	107.2
Tap water	1	0.93	5.33	93.4
	2	2.12	4.20	106.4
	3	3.08	1.52	102.6

In addition, Hg^{2+} in seafood samples was detected to reveal the practical utility of **HMI-Hg^{2+}**. Unexpectedly, there were better linear relationships between the Hg^{2+} concentration and the emission intensity at 585 nm for the three samples (R^2>0.99). The **HMI-Hg^{2+}** spiked recovery of Hg^{2+} in seafood samples was calculated (Table 2). Calculated recoveries were between 96.2% and 102.2%, and the RSD ranged from 0.28% to 3.34%. The results revealed that the **HMI-Hg^{2+}** detection of Hg^{2+} in seafood samples was feasible.

Table 2 Detection results of Hg^{2+} in seafood samples

Sample	Added/ (μmol•L^{-1})	Found/ (μmol•L^{-1})	RSD (n=3)/%	Recovery/%
Fish	2	2.03	1.11	101.3
	4	4.08	3.11	102.0
	6	6.02	0.85	100.4
Shrimp	2	1.92	2.72	96.2
	4	4.01	3.34	100.2
	6	5.87	1.91	97.9
Scallop	2	2.01	0.74	100.4
	4	4.09	0.28	102.2
	6	5.88	1.18	97.9

2.7 Cell imaging and mitochondrial-localization

Fluorescence imaging was carried out in MCF-7 cells to assess the cell permeability and applicability of probe **HMI-Hg^{2+}** in the living cell. The cytotoxicity of **HMI-Hg^{2+}** was investigated, which illustrated that **HMI-Hg^{2+}** was nontoxic in higher concentrations. Therefore, fluorescence imaging experiments were carried out in MCF-7 cells (Figure 8). In the absence of Hg^{2+}, no fluorescence was observed in the green channel of pretreated MCF-7. With further incubation with different Hg^{2+} concentrations, we noticed green fluorescence, and with the increase of the added Hg^{2+} concentration the cell fluorescence brightness was intense. The consequences denoted that **HMI-Hg^{2+}** exhibited good cell membrane permeability and could monitor lower levels of Hg^{2+} in cells.

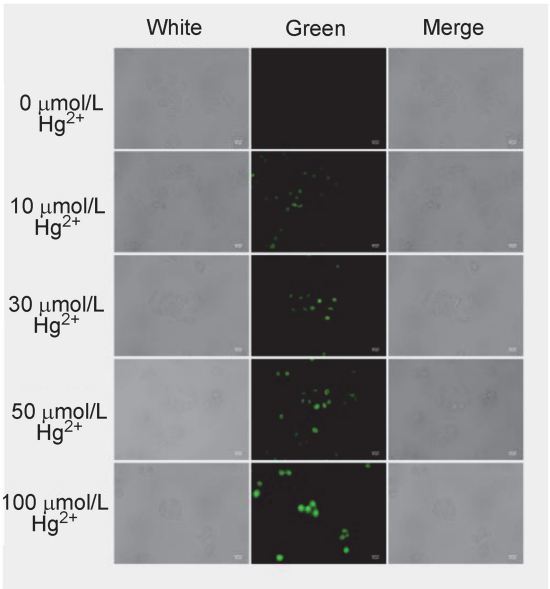

Figure 8 Fluorescence images of MCF-7 cells incubated with **HMI-Hg^{2+}** (10 μmol/L) and different concentrations of Hg^{2+} (0, 10, 30, 50 and 100 μmol/L)
Left: bright field image; middle: green channel image; right: merge field image.

To demonstrate that **HMI-Hg^{2+}** can stain mitochondria, co-localization experiments of **HMI-Hg^{2+}** (10 μmol/L) and Mito-Tracker Green FM in MCF-7 cells were performed. As shown in Figure 9, the fluorescence image of MCF-7 cells with good morphology after co-staining was observed. MCF-7 cells showed strong fluorescence in the red channel (Figure 9B) and green channel (Figure 9C). A practically complete overlap between the two channels (Figure 9D) was observed, nearly the changes in fluorescence intensity in the linear region were the same (Figure 9E), and the intensity scatterplots for the red and green channels were also highly consistent (Figure 9F). In addition, the Pearson's co-localization coefficient used to describe the correlation of the intensity distribution was 0.97, indicating that **HMI-Hg^{2+}** could localize in mitochondria.

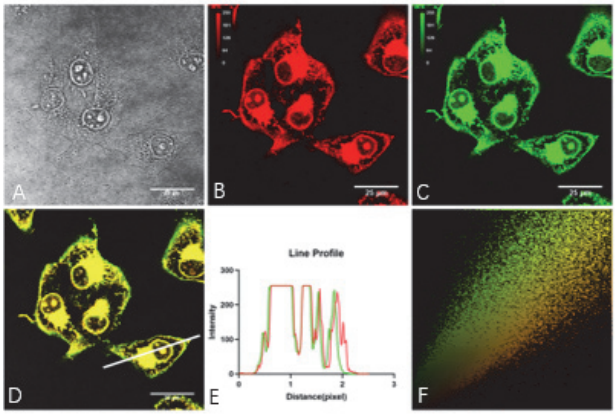

Figure 9 Colocalization experiments of **HMI-Hg^{2+}** and Mito-Tracker Green FM in MCF-7 cells

(A) Bright field image; (B) Red channel image (from **HMI-Hg^{2+}**, the emission was collected at 585 nm with red pseudocolor); (C) Green channel image (from Mito-Tracker Green FM); (D) Merge image of (B) and (C); (E) Intensity distribution of fluorescence intensity changes in red and green channels of MCF-7 cells stained with **HMI-Hg^{2+}** and Mito-Tracker Green FM; (F) Intensities of green and red channels Scatter plot.

2.8 Test strip application

The excellent fluorescence properties of **HMI-Hg^{2+}** in practical samples encouraged us to study its application in test papers. Test papers in absolute ethanol of **HMI-Hg^{2+}** were prepared (1 mmol/L).[32] As shown in Figure 10, the **HMI-Hg^{2+}** test strips without the addition of Hg^{2+} exhibited green fluorescence and gradually transition to orange fluorescence after the dropwise addition of Hg^{2+}, and the luminescence intensity remained stable when the concentration reached 60 nmol/L, indicating that **HMI-Hg^{2+}** had potential applications in the convenient detection of trace Hg^{2+}.

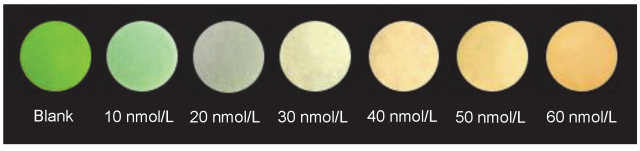

Figure 10 Picture of **HMI-Hg^{2+}** test strips with different concentrations of Hg^{2+} under UV light irradiation (365 nm)

3 Conclusions

In summary, a tun-on fluorescent probe **HMI-Hg^{2+}** was developed for Hg^{2+} sensing and imaging. **HMI-Hg^{2+}** distinguished Hg^{2+} from other metal ions by light pink to yellow color change. Spectroscopic studies showed that **HMI-Hg^{2+}** exhibited excellent selectivity and anti-interference for Hg^{2+} with high sensitivity, rapid response (about 6 s) and low detection limit (0.22 μmol/L). **HMI-Hg^{2+}** could be used to detect Hg^{2+} in water samples and seafood samples. Furthermore, **HMI-Hg^{2+}** could carry out cell staining and imaging experiments. The application of test strips also achieved satisfactory results. It showed that **HMI-Hg^{2+}** could be used as a sensitive sensor and has broad application prospects in practical detection.

4 Experimental section

4.1 General methods

Metal ion stock solutions were prepared with nitrate or hydrochloride in double-distilled water. Stock solution of **HMI-Hg^{2+}** was prepared in DMSO and was further diluted with a mixed solution of DMSO/H_2O (V∶V=5∶5, PBS 20 mmol/L, pH=10.17) to make a final concentration at 10 μmol/L. The solution volume used for optical experiments was 2 mL. Ex slit: 5, Em slit: 10, λ_{ex}: 455 nm, λ_{em}: 585 nm.

4.2 Synthesis of probe HMI-Hg^{2+}

p-Hydroxybenzaldehyde (1.22 g, 10 mmol) and 1,4-dimethylpyridinium iodide (2.35 g, 10 mmol) were added to a 100 mL round bottom flask, and 40 mL of absolute ethanol was added to completely dissolve it. After adding two drops of piperidine, the mixture was refluxed for 16 h, filtered after the reaction, and washed with ice-ethanol three times to obtain compound **1**[33] with a yield of 85% (2.88 g, 8.5 mmol). m.p. 194～196 ℃; ^{1}H NMR (400 MHz, DMSO-d_6) δ: 8.67 (s, 2H), 8.03 (s, 2H), 7.87 (d, J=13.9 Hz, 1H), 7.53 (d, J=5.5 Hz, 2H), 7.14 (d, J=14.0 Hz, 1H), 6.74 (d, J=5.3 Hz, 2H), 4.15 (s, 3H); ^{13}C NMR (101 MHz, DMSO-d_6) δ: 163.09, 153.14, 144.43, 141.66, 130.57, 124.48, 122.28, 117.99, 116.79, 46.36.

Compound **1** (1.36 g, 4 mmol) and hexamethylenetetramine (0.9 g, 6.4 mmol) were dissolved in trifluoroacetic acid (25 mL), and the reaction was monitored by TLC plate until the consumption of starting material was complete. After cooling to room temperature, HCl (1 mol/L, 50 mL) was added to the mixture, which was then stirred until precipitation occurred. After filtration, a yellow powder compound **HMI-CHO** (0.81 g, 2.2 mmol) was obtained with a yield of 55% (synthesis of **HMI-CHO** regarding existing methods[34]). ^{1}H NMR (400 MHz, DMSO-d_6) δ: 11.43 (s, 1H), 10.34 (s, 1H), 8.83 (d, J=6.4 Hz, 2H), 8.17 (d, J=6.5 Hz, 2H), 8.03 (d, J=16.4 Hz, 1H), 8.01 (d, J=6 Hz, 1H), 7.92 (d, J=8.7 Hz, 1H), 7.40 (d, J=16.4 Hz, 1H), 7.15 (d, J=8.6 Hz, 1H), 4.23 (s, 3H); ^{13}C NMR (101 MHz, DMSO-d_6) δ: 190.73, 162.73, 153.02, 145.42, 140.59, 135.73, 129.19, 127.27, 123.61, 123.15, 121.89, 118.72, 47.15; HRMS (ESI$^+$) calcd. for $C_{15}H_{14}NO_2$ [M－I]$^+$ 240.1019,

found 240.1018.

HMI-Hg^{2+} was synthesized according to an existing method.[35] m.p. 195.6～197.9 ℃; ^{1}H NMR (400 MHz, DMSO-d_6) δ: 12.28 (s, 2H), 10.66 (s, 1H), 8.78 (d, J=4.9 Hz, 2H), 8.18 (d, J=4.9 Hz, 2H), 7.97 (d, J=16.2 Hz, 1H), 7.78 (s, 1H), 7.57 (d, J=8.3 Hz, 1H), 7.26 (d, J=15.9 Hz, 1H), 6.95 (d, J=8.1 Hz, 1H), 5.46 (s, 1H), 4.21 (s, 3H), 2.85～2.54 (m, 8H); ^{13}C NMR (101 MHz, DMSO-d_6) δ: 172.89, 156.30, 152.97, 144.78, 142.25, 129.16, 128.76, 127.45, 126.66, 122.97, 120.09, 116.09, 46.70, 44.94, 34.16, 27.25; HRMS (ESI$^+$) calcd. for $C_{21}H_{24}NO_5S_2$ [M−I]$^+$ 434.1090, found 434.1088.

4.3 Preparation of actual samples testing solution

Tap water and lake water were taken from Bohai University. The actual water samples were filtered, boiled and then used to prepare a mixed solution of DMSO/H_2O (V∶V=5∶5). Then, the two samples were spiked with different concentrations of Hg^{2+} (0～5 μmol/L).

0.5 g of fish, shrimp and scallop samples were pretreated and placed in a beaker, poured into concentrated nitric acid (10 mL), and then sonicated overnight. After cooling to room temperature, the reaction mixture was centrifuged. The pH of the supernatant was adjusted to 7.4 with NaOH solution, and the volume was made up to 50 mL with double-distilled water.

Supporting Information Structural characterization of compound **1**, **HMI-CHO** and **HMI-Hg^{2+}**, and fluorescence spectra related to this paper. The Supporting Information is available free of charge via the Internet at http://sioc-journal.cn.

References

[1] Liu, L.; Ma, J.; Pan, J.; Li, D.; Wang, H.; Yang, H. *New J. Chem.* **2021**, *45*, 5049.
[2] Samanta, T.; Das, N.; Patra, D.; Kumar, P.; Shunmugam, R. *ACS Sustainable Chem. Eng.* **2021**, *14*, 5196.
[3] Okpala, C. O. R.; Sardo, G.; Vitale, S.; Bono, G.; Arukwe, A. *Crit. Rev. Food Sci.* **2018**, *58*, 1986.
[4] Ding, J.; Li, H.; Xie, Y.; Peng, Q.; Li, Q.; Li, Z. *Polym. Chem.* **2017**, *8*, 2221.
[5] Ullah, A.; Ali, I.; Ahmed, F.; Khan, S.; Shah, M. R.; Shaheen, F. *J. Mol. Liq.* **2019**, *296*, 112095.
[6] García-Calvo, J.; Vallejos, S.; García, F. C.; Rojo, J.; García, J. M.; Torroba, T. *Chem. Commun.* **2016**, *52*, 11915.
[7] Das, S.; Sarkar, A.; Rakshit, A.; Datta, A. *Inorg. Chem.* **2018**, *57*, 5273.
[8] Tian, M.; Wang, C.; Ma, Q.; Bai, Y.; Sun, J.; Ding, C. *ACS Omega* **2020**, *5*, 18176.
[9] Chen, C.-G.; Vijay, N.; Thirumalaivasan, N.; Velmathi, S.; Wu, S.-P. *Spectrochim. Acta*, *Part A* **2019**, *219*, 135.
[10] Shan, Y.; Yao, W.; Liang, Z.; Zhu, L.; Yang, S.; Ruan, Z. *Dyes Pigm.* **2018**, *156*, 1.
[11] Harris Hugh, H.; Pickering Ingrid, J.; George Graham, N. *Science* **2003**, *301*, 1203.
[12] Pan, Z.; Xu, Z.; Chen, J.; Hu, L.; Zhang, J. *J. Fluoresc.* **2020**, *30*, 505.
[13] Caballero, A.; Lloveras, V.; Curiel, D.; Tárraga, A.; Espinosa, A.; García, R.; Vidal-Gancedo, J.; Rovira, C.; Wurst, K.; Molina, P.; Veciana, J. *Inorg. Chem.* **2007**, *46*, 825.
[14] Li, Y.; Chen, C.; Li, B.; Sun, J.; Wang, J.; Gao, Y.; Zhao, Y.; Chai, Z. *J. Anal. Atom Spectrom.* **2006**, 21, 94.
[15] Li, Q.; Zhang, Z.; Wang, Z. *Anal. Chim. Acta* **2014**, *845*, 7.
[16] Tang, L.; Yu, H.; Zhong, K.; Gao, X.; Li, J. *RSC Adv.* **2019**, *9*, 23316.
[17] Kan, C.; Wu, L.; Shao, X.; Wang, X.; Zhang, Y.; Zhu, J.; Qiu, S. *Tetrahedron Lett.* **2020**, *61*, 152407.
[18] Lu, M.; Qiu, S.; Cui, S.; Pu, S. *Tetrahedron Lett.* **2020**, *61*, 152372.
[19] Duan, Q.; Lv, X.; Liu, C.; Geng, Z.; Zhang, F.; Sheng, W.; Wang, Z.; Jia, P.; Li, Z.; Zhu, H.; Zhu, B. *Ind. Eng. Chem. Res.* **2019**, *58*, 11.
[20] Xu, D.; Tang, L.; Tian, M.; He, P.; Yan, X. *Tetrahedron Lett.* **2017**, *58*, 3654.
[21] Tang, L.; Zhou, L.; Yan, X.; Zhong, K.; Gao, X.; Li, J. *J. Photochem. Photobiol*., *A* **2020**, 387, 112160.
[22] Zhang, W.; Yu, C.; Yang, M.; Wen, S.; Zhang, J. *Molecules* **2021**, *26*, 3385.
[23] Huang, L.; Yang, Z.; Zhou, Z.; Li, Y.; Tang, S.; Xiao, W.; Hu,M.; Peng, C.; Chen, Y.; Gu, B.; Li, H. *Dyes Pigm.* **2019**, *163*, 118.
[24] Liu, B.; Liu, J.; He, J.; Zhang, J.; Zhou, H.; Gao, C. *Chem. Phys.* **2020**, 539, 110944.
[25] Gao, Q.; Jiao, Y.; He, C.; Duan, C. *Molecules* **2019**, *24*, 2268.
[26] Xu, J.; Wang, Z.; Liu, C.; Xu, Z.; Wang, N.; Cong, X.; Zhu, B. *Luminescence* **2018**, *33*, 1122.
[27] Cheng, X.; Li, Q.; Qin, J.; Li, Z. *ACS Appl. Mater. Interfaces* **2010**, *2*, 1066.
[28] Chang, I. J.; Hwang, K. S.; Chang, S.-K. *Dyes Pigm.* **2017**, *137*, 69.
[29] Pan, J.; Ma, J.; Liu, L.; Li, D.; Huo, Y.; Liu, H. *J. Photochem. Photobiol*., *A* **2021**, *416*, 113322.
[30] Tang, L.; Sun, Y.; Zhong, K.; Jin, L. *Tetrahedron Lett.* **2020**, *61*, 152470.
[31] Li, F.; Zhong, K.; Hou, S.; Tang, L.; Bian, Y. *Tetrahedron Lett.* **2020**, *61*, 151558.
[32] Huang, L.; Sheng, W.; Wang, L.; Meng, X.; Duan, H.; Chi, L. *RSC Adv.* **2021**, *11*, 23597.
[33] Brooker, L. G. S; Keyes, G. H.; Heseltine, D. W. *J. Am. Chem. Soc.* **1951**, *73*, 5350.
[34] Chen, G.; Zhou, W.; Zhao, C.; Liu, Y.; Chen, T.; Li, Y.; Tang, B. *Anal. Chem.* **2018**, *90*, 12442.
[35] Madhu, S.; Josimuddin, S.; Ravikanth, M. *New J. Chem.* **2014**, *38*, 3770.

(Zhao, C.)

